

## Electronic Structure of Ultrasmall Quantum-Well Boxes

Garnett W. Bryant

*McDonnell Douglas Research Laboratories, St. Louis, Missouri 63166*

(Received 11 May 1987)

The electronic structure of interacting, few-electron systems confined in quasi-zero-dimensional, ultrasmall, quantum-well boxes has been calculated by use of the multielectron effective-mass Schrödinger equation. The configuration-interaction method is used to include electron correlation. Correlation effects are dominant in large boxes; the electrons form a Wigner lattice. In smaller boxes subband spacing becomes dominant and the carriers become frozen in the lowest subbands. The calculations determine how and on what size scale this transition occurs.

PACS numbers: 73.20.Dx, 71.45.Lr

Individual atoms are the microscopic limit for very small, confined-electron systems, in which the motion in all three spatial dimensions is quantized. Bulk systems bounded by surfaces are the macroscopic limit for very large, confined-electron systems. Recently, systems in the intermediate, mesoscopic regime, where the crossover from atomic to bulk behavior occurs, have begun to receive attention. Studies<sup>1-5</sup> of semiconductor microcrystallites, with dimensions  $L$  from one to several tens of nanometers, extend the investigation of carrier-confinement effects away from the atomic limit. With the recent advances in the art of microfabrication, ultrasmall ( $0.02 \mu\text{m} \lesssim L \lesssim 0.5 \mu\text{m}$ ) quasi-zero-dimensional quantum-well boxes can be made<sup>6-9</sup> which exhibit carrier confinement, extending the investigations away from the macroscopic limit and into the submicrometer size regime. The properties of ultrasmall structures are governed by the physics of the mesoscopic regime. Because ultrasmall structures give promise of novel, device applications,<sup>10,11</sup> there is strong motivation to develop quickly an understanding of mesoscopic physics.

The carriers in a bulk ( $L \gtrsim 1.0 \mu\text{m}$ ) structure form a many-electron system of weakly interacting particles which can be modeled by the single-particle effective-mass equation. In ultrasmall structures ( $L \lesssim 0.1 \mu\text{m}$ ) the effective-mass approach still provides a good description of the motion through the lattice. However, the carriers cannot be assumed to be a weakly correlated many-particle system. Consider a quantum box constructed with use of the confinement at an interface to define one of the confined dimensions. For a typical inversion-layer charge density of  $10^{11} \text{ cm}^{-2}$ , a two-dimensional uniform gas in a square,  $0.1\text{-}\mu\text{m}$ -wide box would contain ten carriers; in a box  $0.01 \mu\text{m}$  wide, less than one carrier. Carriers in ultrasmall boxes must be treated as interacting few-particle systems. In this Letter I calculate the electronic structure of interacting, few-particle systems confined in ultrasmall quantum-well boxes to determine how and on what size scale the carriers in ultrasmall structures become correlated.

The few-particle ( $N \leq 6$ ) systems have been studied<sup>12</sup> by solving the multiparticle effective-mass Schrödinger

equation for two-dimensional, interacting particles confined in a box modeled as a strictly two-dimensional quantum well. No effects of inversion-layer width are included. For simplicity the well is rectangular and has infinite barriers. Because the barriers are infinite, a basis set of wave functions which are separable in the two directions that define the well can be used. The single-particle one-dimensional eigenstates (sines and cosines) are used as the basis functions.

The particle interaction is the Coulomb interaction screened by the background dielectric constant. The correlations are included by use of a configuration-interaction approach. The multiparticle wave function is expanded in terms of Slater determinants constructed from the single-particle noninteracting eigenstates. The kinetic-energy and interaction matrix elements are found by use of the Slater-determinant basis and the Hamiltonian is diagonalized to find the eigenstates. The evaluation of the Coulomb matrix elements is straightforward.<sup>13</sup>

In the infinite-barrier model, all kinetic-energy matrix elements scale as  $1/L^2$  and all interaction matrix elements scale as  $1/L$  when the dimension  $L$  of the box is changed without changing the box shape. This scaling determines the nature of the electron system. For small  $L$ , the Coulomb interactions are insignificant compared to the single-particle level spacings; the electrons are independent, uncorrelated, particles. As  $L$  increases, the interactions become significant and the multielectron states become correlated. The multielectron states evolve continuously, as  $L$  increases, from the exact, independent-particle states of the small- $L$  limit. In the infinite-barrier model, the results are independent of the electron mass  $m_e$  and dielectric constant  $\epsilon$  if all energies are scaled by the effective Rydberg,  $R_e = e^2 m_e / 2a_0^2 \epsilon^2$ , and the lengths are scaled by the effective Bohr,  $a_e = a_0 e / m_e$ . To illustrate the important size scales, I present results for GaAs wells,  $m_e = 0.067m_0$  and  $\epsilon = 13.1$ . The lengths are scaled by  $a_0$  and energies by  $R_e$ .

The evolution of the energy levels of an interacting, confined system that occurs when the box size changes is shown in Figs. 1 and 2 for two simple systems: two in-

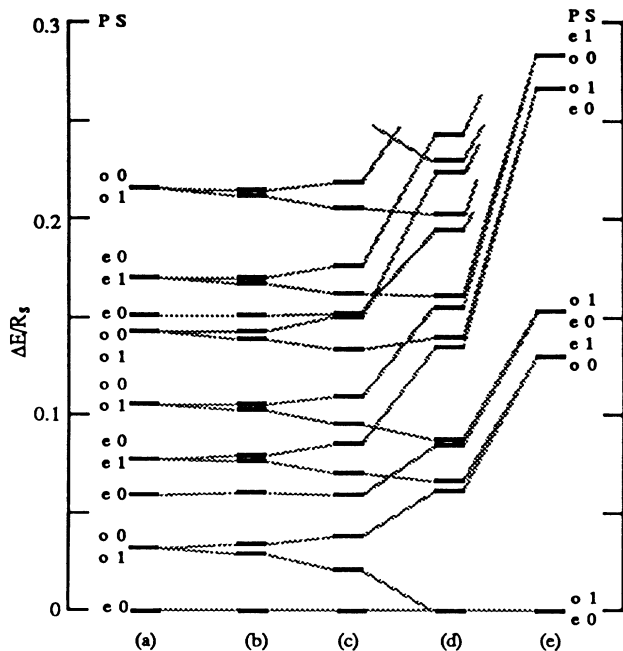


FIG. 1. Energy levels for two electrons in a long, narrow ( $L_y = 10L_x$ ) GaAs quantum-well box. The spacings are measured relative to the ground-state energy  $E_g$  and scaled by  $R_s$ . (a) For noninteracting electrons  $L_y = 20a_0$ ,  $E_g = 1.905R_s$ , and  $R_s = 10^5 \times R_e$ . For interacting electrons  $L_y/a_0$ ,  $E_g/R_s$ , and  $R_s/R_e$  are (respectively) (b) 20, 1.907,  $10^5$ ; (c) 200, 1.923,  $10^3$ ; (d) 2000, 1.987, 10; and (e)  $2 \times 10^4$ , 2.314, 0.1. The parity  $P$  (e = even, o = odd) and total spin  $S$  of each state are indicated.

interacting carriers in (a) long, narrow ( $L \equiv L_y = 10L_x$ ) quantum boxes (Fig. 1) and (b) square quantum boxes (Fig. 2). The energies are scaled by a factor  $R_s$  which is different for each  $L$  to account for the  $1/L^2$  scaling of the kinetic energies.<sup>14</sup> If the Coulomb interactions were unimportant, then the scaled energy levels would be independent of  $L$ . The increases in the scaled ground-state energy and the changes in the level spacings that occur as  $L$  increases show how important the electron-electron interaction becomes in large boxes.

The internal motion of electrons in long, narrow structures is quasi one dimensional because the carriers are in the lowest subband of the narrow ( $x$ ) direction. Mixing of higher  $x$  subbands is insignificant in the size regime covered in Fig. 1. Ten  $y$  subbands were used to account for correlations along the long direction. Energies calculated with 10  $y$  subbands differ from energies calculated with 8  $y$  subbands by less than 0.1%. The internal motion in the square box is two dimensional. Six  $x$  and six  $y$  subbands were used to obtain energies accurate to 0.1% in square boxes. The effective Coulomb interaction increases as the dimensionality is lowered.<sup>15</sup> The Coulomb contribution to the ground-state energy  $E_g$  is larger, when measured on a common energy scale, in a

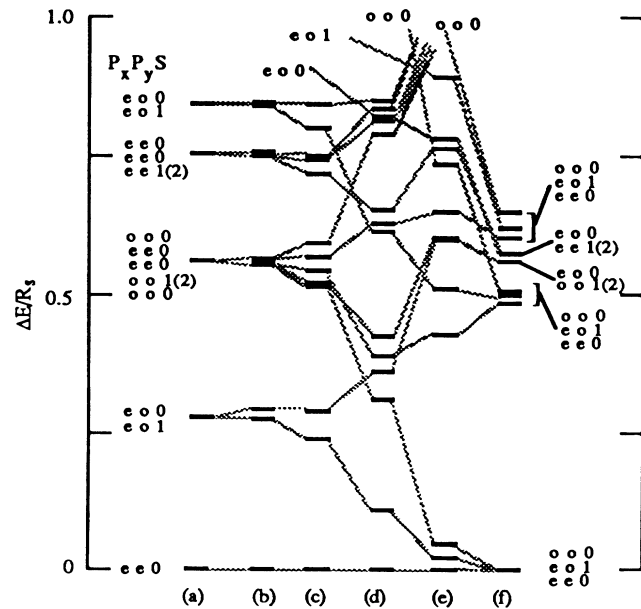


FIG. 2. Energy levels for two electrons in a square GaAs quantum-well box.  $L_y/a_0$ ,  $E_g/R_s$ , and  $R_s/R_e$  are (respectively) (a) for noninteracting electrons, 20, 0.377,  $10^4$ ; and for interacting electrons, (b) 20, 0.387,  $10^4$ ; (c) 200, 0.456,  $10^2$ ; (d) 2000, 0.996, 1; (e)  $2 \times 10^4$ , 3.925, 0.01; and (f)  $6 \times 10^4$ , 4.373, 0.0022. The  $x$  and  $y$  parity and total spin of each state are indicated. States with odd- $x$ , even- $y$  parity are degenerate with even- $x$ , odd- $y$  parity states and are not shown. Additional degeneracies not due to parity or spin are shown in parentheses.

long, narrow box than in a square box with the same long ( $L_y$ ) dimension.

For  $L_y \lesssim 1$  nm, the scaled energy levels shift slightly from the noninteracting levels, and exchange splitting occurs. Typically, states with total spin  $S=1$  have lower energy (Hund's rule) than  $S=0$  states with the same parity. When  $L_y \approx 10$  nm, the scaled energy levels shift substantially from the levels of the noninteracting system and have begun to cross in long, narrow boxes. Significant Coulomb contributions to  $E_g$  begin to occur on this length scale. When  $L_y \approx 100$  nm, substantial reordering of the levels occurs in both square boxes and long, narrow boxes.

In the large- $L$  limit, where interactions dominate the kinetic energy, the system should become strongly correlated, with the electrons located to minimize the repulsive interaction as in a Wigner lattice (WL) for unconfined systems. The signature of the WL states in a confined system is the degeneracy of the levels. For example, in a long, narrow box there is one way to put two particles with the same spin on the box axis to minimize the direct Coulomb interaction. For two particles with opposite spin, there are two configurations. In a square box the particles would sit on opposite ends of the same diagonal in the WL limit. The degeneracy would be double the degeneracy for a long, narrow box since there

are two equivalent diagonals. In long, narrow boxes, the evolution of the states into levels with the degeneracies of the WL limit<sup>16</sup> occurs when  $L \gtrsim 0.1 \mu\text{m}$  and the splitting of levels that are degenerate in the WL limit is no longer apparent. The WL limit is reached at larger  $L$  for square boxes because the effective Coulomb interaction is weaker. Ceperly<sup>17</sup> found that a two-dimensional electron gas becomes a WL when  $r_s > 33a_e$ . In GaAs the WL would occur for  $r_s > 0.34 \mu\text{m}$ . This is consistent with the length scale on which the confined square system approaches the WL limit.

The evolution of the energy levels is more complicated for systems with more than two particles. When  $N > 2$  the level mixing is more complex, degeneracies in the WL limit are higher, and the transition to the WL limit occurs at larger  $L$ , requiring more accurate calculations to reach the WL limit. I calculated the cases of three and four particles in long, narrow boxes with accuracy adequate for tracing the evolution to the WL limit. For square boxes, the level degeneracies of the WL limit are not obvious when the number of particles is incommensurate with the symmetry of the structure; for example, when a square box contains three particles. The present results suggest that three spin-parallel electrons in a square box have four degenerate states in the WL limit. This is the degeneracy expected from the symmetry of the box. However, I have not yet been able to calculate with adequate accuracy the states for two parallel- and one opposite-spin particle to confirm that the degeneracy in the WL limit is twelve, as needed to be consistent with the results for parallel-spin particles.

The spatial correlations of two particles in square boxes is shown in Fig. 3. For boxes in which the confining potential dominates, the carrier density  $\sigma(r)$  approaches the independent-carrier density. As  $L$  increases, the carriers move apart along the diagonals with  $\sigma(r)$  peaking farther from the center, and the density on the diagonals increases relative to the density off the diagonals. In addition, as  $L$  increases, the particle positions become more strongly correlated. As  $L$  increases, the probability,  $\sigma(\mathbf{r}, \mathbf{r}_0)$ , for finding one particle at  $\mathbf{r}$  if the second is on a diagonal at  $\mathbf{r}_0$  increases for  $\mathbf{r}$  at the opposite end of the same diagonal and decreases for other  $\mathbf{r}$ .

The multiparticle wave functions evolve, as  $L$  increases, from the single-configuration Slater-determinant states of the noninteracting system by a mixing in of other configurations with the same parity and spin. For  $L \lesssim 0.01 \mu\text{m}$ , the only important configuration (probability  $\gtrsim 0.95$ ) in the interacting ground state is the noninteracting ground-state configuration. For  $L \gtrsim 0.1 \mu\text{m}$ , the excited noninteracting configurations are mixed in with comparable or greater probability than the noninteracting ground state. The important excited configurations of an infinite-barrier confined system are different from those of an atomic system. In an atom the excited single-particle levels get closer together (like

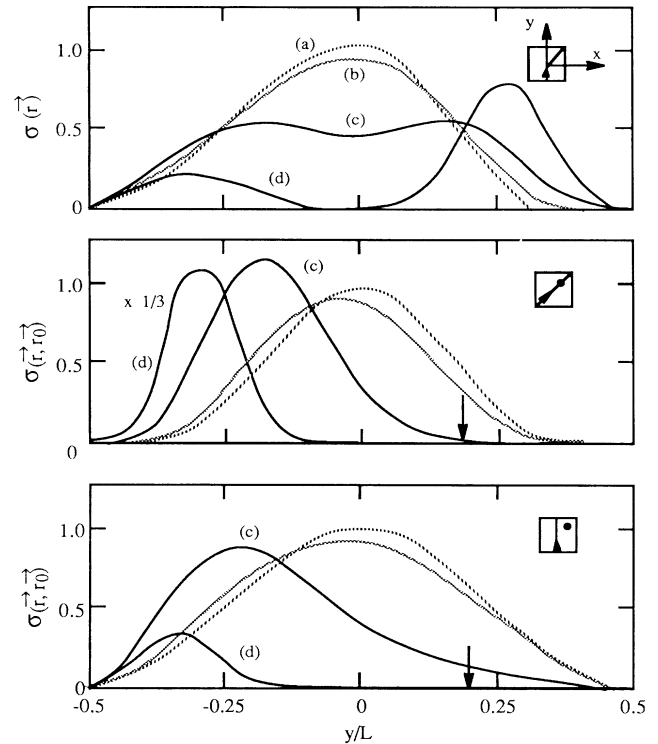


FIG. 3. Ground-state single-particle density  $\sigma(r)$  and the two-particle conditional density  $\sigma(r, r_0)$  for two particles in a square box: (a) for noninteracting particles; and for interacting particles, (b)  $L=200a_0$ , (c)  $L=2000a_0$ , and (d)  $L=20000a_0$ . The paths in the insets define the contours on which the densities are determined. The dot in the inset and the arrow on the axis indicate the position  $r_0$ . The densities are scaled for each  $L$  so that the densities of the noninteracting states are independent of  $L$ .

$1/n^2$ ) as the excitation level  $n$  increases, and the most important excited configurations in an atomic correlated state are the single-particle excitations from the highest filled level. In contrast, the excited single-particle levels of the infinite-barrier box get farther apart (like  $n^2$ ) as the excitation level increases, and the most important excited states in a correlated state are excitations to the lowest empty level. To conserve parity, such excitations must be two-particle excitations from the highest filled level or single-particle excitations from deeper in the core. For three- and four-particle systems, the most probable excited configurations are those with empty cores and those with unpaired spins in the core.

In small ( $L \lesssim 0.01 \mu\text{m}$ ) infinite-barrier boxes the correlations are weak. However, the importance of Coulomb interactions in small boxes defined by finite barriers is underestimated by the present model because the infinite-barrier model overestimates the competing kinetic-energy effects. In boxes defined by finite barriers, correlation effects should extend to smaller size scales, and Coulomb repulsion should inhibit the pairing

of electrons. For example, in the smallest square box ( $L \approx 1$  nm) considered in Fig. 2, the energy cost to pair two electrons is  $0.01R_s = 5.3$  eV, more than any realistic finite barrier in a GaAs structure.

In conclusion, particle-particle correlations occur on the mesoscopic length scale in quantum microstructures. The correlations are a few-particle, rather than a many-particle, effect. As a consequence, these structures display a rich variety of electronic properties—unpaired electrons, weakly correlated states, and confined Wigner lattice states—that make microstructures intriguing systems to study.

This work was performed under the McDonnell Douglas Independent Research and Development program.

<sup>1</sup>C. J. Sandroff, D. M. Hwang, and W. M. Chung, *Phys. Rev. B* **33**, 5953 (1986).

<sup>2</sup>J. Warnock and D. D. Awschalom, *Appl. Phys. Lett.* **48**, 425 (1986).

<sup>3</sup>L. Brus, *IEEE J. Quantum Electron.* **22**, 1909 (1986), and references therein.

<sup>4</sup>H. M. Schmidt and H. Weller, *Chem. Phys. Lett.* **129**, 615 (1986).

<sup>5</sup>Y. Kayanuma, *Solid State Commun.* **59**, 405 (1986).

<sup>6</sup>M. A. Reed, R. T. Bate, K. Bradshaw, W. M. Duncan, W. R. Frensley, J. W. Lee, and H. D. Shih, *J. Vac. Sci. Tech-*

*nol. B* **4**, 358 (1986).

<sup>7</sup>K. Kash, A. Scherer, J. M. Worlock, H. G. Craighead, and M. C. Tamargo, *Appl. Phys. Lett.* **49**, 1043 (1986).

<sup>8</sup>J. Cibert, P. M. Petroff, G. J. Dolan, S. J. Pearton, A. C. Gossard, and J. H. English, *Appl. Phys. Lett.* **49**, 1275 (1986).

<sup>9</sup>H. Temkin, G. J. Dolan, M. B. Panish, and S. N. G. Chu, *Appl. Phys. Lett.* **50**, 413 (1987).

<sup>10</sup>T. Inoshita, S. Ohnishi, and A. Oshiyama, *Phys. Rev. Lett.* **57**, 2560 (1986).

<sup>11</sup>M. Asada, Y. Miyamoto, and Y. Suematsu, *IEEE J. Quantum Electron.* **22**, 1915 (1986).

<sup>12</sup>A preliminary report on these calculations was given as part of G. W. Bryant, D. B. Murray, and A. H. MacDonald, in "Superlattices and Microstructures," Proceedings of the Second International Conference on Superlattices, Microstructures and Microdevices, Göteborg, Sweden, 1986 (to be published).

<sup>13</sup>G. W. Bryant, *Phys. Rev. B* **31**, 7812 (1985).

<sup>14</sup> $R_s$  scales as  $1/L_y^2$  except for case (f) in Fig. 2. In that case,  $R_s$  was chosen to be factor of 2 larger than would be obtained for  $1/L_y^2$  scaling, so that the scaled energy levels would fit on the figure. In Fig. 2(f) the energy-level spacings would be twice as large if  $1/L_y^2$  scaling was used.

<sup>15</sup>G. W. Bryant, *Phys. Rev. B* **29**, 6632 (1984).

<sup>16</sup>To see that the correct degeneracies are obtained in the WL limit, one must remember that the levels are independent of  $s_z$ , so that each  $S=1$  level has three degenerate levels ( $s_z = \pm 1, 0$ ), and that the odd- $x$ , even- $y$  parity states are not shown in Fig. 2.

<sup>17</sup>D. Ceperley, *Phys. Rev. B* **18**, 3126 (1978).